Observational Study

Medicine®

OPEN

Histogram analysis with computed tomography angiography for discriminating soft tissue sarcoma from benign soft tissue tumor

Gang Wu, MD[a], Ruyi Xie, MD[a,*], Yitong Li, MD[a], Bowen Hou, MD[a], John N. Morelli, MD[b], Xiaoming Li, PhD[a]

Abstract

To investigate the feasibility of histogram analysis with computed tomography angiography (CTA) in distinguishing between soft tissue sarcomas and benign soft tissue tumors. Fourty nine patients (23 men, mean age = 44.3 years, age range = 25–64) with pathologically-confirmed soft tissue sarcoma (n = 24) or benign soft tissue tumors (n = 25) in the lower extremities undergoing CTA for tumor evaluation were retrospectively analyzed. Two radiologists separately performed histogram analyses of CT density with CTA images by drawing a region of interest (ROI). The 10th (P10), 25th (P25), 50th (P50), 75th (P75), 90th percentiles (P90), mean, and standard deviations (SD) of measured tumor density were obtained along with measurements of the absolute value of kurtosis (AVK), absolute value of skewness (AVS), and inhomogeneity for each tumor. Intra-class correlation coefficients (ICC) were calculated to determine inter- and intra-reader variability in parameter measurements. The Mann–Whitney *U* test was used to compare histogram parameters between soft tissue sarcomas and benign soft tissue tumors. Receiver operator characteristic (ROC) curves were constructed to evaluate the accuracy of tumor discrimination. ICC was greater than 0.7 for AVS, AVK, and inhomogeneity, and >0.9 for mean, SD, and all percentile measures. There was no significant difference in P10, P25, P50, P75, P90, mean, or SD between soft tissue sarcomas and benign tumors ($P > .05$). AVS, AVK, and inhomogeneity were significantly higher in soft tissue sarcomas ($P < .05$). Areas under the curve (AUC) were 0.81, 0.83, and 0.84 for AVS, AVK, and inhomogeneity respectively. AUC were below 0.6 for mean, SD, and all percentiles.

Skewness, kurtosis, and inhomogeneity measurements derived from histogram analysis from CTA distinguish between soft tissue sarcomas and benign soft tissue tumors.

Abbreviations: AUC = area under curve, AVK = absolute value of kurtosis, AVS = absolute value of skewness, CT = computed tomography, CTA = computed tomography angiography, CTTA = computed tomography texture analysis, ICC = intra-class correlation coefficient, ROC = receiver operator characteristic, ROI = region of interest, SD = standard deviation.

Keywords: computed tomography angiography, histogram analysis, inhomogeneity, soft tissue sarcoma, soft tissue tumor

1. Introduction

Computed tomography (CT) is often not the preferred modality for imaging extremity soft tissue tumors due to poor contrast resolution.[1,2] However, recent studies have found that computed tomography texture analysis (CTTA) can identify and quantify tumor spatial heterogeneity.[3–7] Histogram analysis of CT density, one of the most widely used CTTA methods, has been reported to distinguish between benign and malignant lesions[8–10] based on differences in heterogeneity. Compared with non-contrast CT, contrast enhanced CT may be more useful for histogram analysis of density, as tissue CT attenuation and spatial heterogeneity are increased with the latter.[11–13]

Computed tomography angiography (CTA) is frequently used for evaluating soft tissue masses in the lower extremity, as it can provide information regarding blood supply and vascular invasion.[14,15] CTA is often a preoperative requirement for large soft tissue tumors to assess regional vascular invasion.[16,17] In addition, CTA can determine the number of feeding arteries, which is valuable in distinguishing between benign and malignant soft tissue tumors, the latter which tend to have more feeding arteries.[18] As with conventional contrast-enhanced CT, CTA is more suitable than non-contrast CT for histogram analysis.[19]

Soft tissue sarcomas in the lower extremity generally have an inhomogeneous density distribution due to complex pathological changes including bleeding, necrosis, and calcification.[20,21] In distinction, benign soft tissue tumors typically have a simple structure and more homogeneous density distributions.[22] We here hypothesize: histogram analysis with CTA can identify and quantify tumor heterogeneity and that benign soft tissue tumors and soft tissue sarcomas differ in spatial heterogeneity. The purpose of the study is therefore to investigate the feasibility of histogram analysis with CTA in distinguishing between soft tissue sarcomas and benign soft tissue tumors.

Editor: Jianxun Ding.

This study has received funding by National Natural Scientific foundation of China (Number: 81801663, 31630025, and 81571643).

The authors have no conflicts of interest to disclose.

[a] Department of Radiology, Tongji Hospital, Tongji Medical College, Huazhong University of Science and Technology, Wuhan, China, [b] St. John's Medical Center Tulsa, Oklahoma.

[*] Correspondence: Ruyi Xie, No. 1095, Jiefang Road, Wuhan, Hubei, 430030, China (e-mail: 42292815@qq.com).

How to cite this article: Wu G, Xie R, Li Y, Hou B, Morelli JN, Li X. Histogram analysis with computed tomography angiography for discriminating soft tissue sarcoma from benign soft tissue tumor. Medicine 2020;99:2(e18742).

Received: 9 August 2019 / Received in final form: 24 November 2019 / Accepted: 16 December 2019

http://dx.doi.org/10.1097/MD.0000000000018742

2. Methods

2.1. Patients

This retrospective study was approved by the Institutional Review Broad of our university. Inform consent was obtained from each patient before study. Inclusion criteria were patients with a pathologically-confirmed benign lower extremity soft tissue tumor or soft tissue sarcoma; patients with a lower extremity CTA examination performed for tumor evaluation. Exclusion criteria were tumors containing predominantly fat, such as lipomas and seriously calcified tumor with calcified scope >30%. Sixty patients from March 2013 to October 2018 were enrolled in this study. Exclusion of patients was as follows: tumors with fat (n=7); seriously calcified tumors (n=4). Thus, a total of 49 patients with soft tissue tumors were analyzed.

2.2. CTA examinations

All CTA examinations were performed on a 128-row CT scanner (Discovery HD 750, GE Healthcare, Milwaukee, WI, USA). The main scan parameters were as follows: tube voltage, 100 kV; tube current, 150 mA; pitch, 0.984:1; thickness, 0.625 mm; field of view, 50 cm. The contrast agent was injected through the antecubital vein by an automatic injector. The flow rate was 3 mL/s. A region of interest (ROI) was drawn at the aortic bifurcation for tracking. Image acquisition automatically began 5.5 seconds after the attenuation in the ROI reached a threshold of 120 Hounsfield units (HU).

2.3. Pathology results

The 49 soft tissue tumors were divided into 2 groups according to the 2013 WHO classification of bone and soft tissue tumors: the soft tissue sarcoma group and benign soft tissue tumor group. The pathology types for soft tissue sarcoma group (n=24) were as follows: synovial sarcoma (n=4), fibrosarcoma (n=7), rhabdomyosarcoma (n=5), leiomyosarcoma (n=3), epithelioid sarcoma (n=2), and hemangiosarcoma (n=3). The pathology types for benign soft tissue tumor group (n=25) were as follows: fibroma (n=9), schwannoma (n=5), hemangioma (n=7), intramuscular myxoma (n=2), and tenosynovial giant cell tumor (n=2).

2.4. Data analysis

Two radiologists with 8 and 9 years' experience in orthopedic oncologic imaging separately performed a histogram analysis of CT density by drawing an ROI on CT source images using Firevoxel. The radiologist with 8 years' experience was asked to perform a second analysis for all cases after an interval of 4 weeks. The ROIs were drawn in different areas on the slice where the tumor size was the greatest. Histogram derived parameters were as follows: 10th percentile (P10), 25th percentile (P25), 50th percentile (P25), 75th percentile (P75), 90th percentile (P90), mean, standard and deviation (SD) of measured tumor density as well as skewness, kurtosis, and inhomogeneity. Absolute values were obtained for skewness and kurtosis (AVS and AVK, respectively).

2.5. Statistical analysis

All statistical analysis was performed using SPSS 21.0 (SPSS Inc., Chicago, IL, USA). Intra-class correlation coefficients (ICC) were calculated to determine inter- or intra-reader variability in parameter measurements. ICC above 0.7 were considered excellent reproducibility. ICC below 0.4 were considered poor reproducibility. ICC between 0.4 and 0.7 were considered acceptable. Histogram parameters were compared between the 2 groups using a Mann–Whitney *U* test. The non-paired student's *t* test was used to compare patient ages between the 2 groups. The chi-square test was used to identify sex differences between the 2 groups. Receiver operator characteristic (ROC) curves were constructed for determining the ability to distinguish benign and malignant tumors. *P*-values <.05 were considered statistically significant.

3. Results

3.1. Reproducibility of measurement

Inter-reader ICC was >0.7 for AVS, AVK, and inhomogeneity, and >0.9 for P10, P25, P50, P75, P90, mean, and SD (see Table 1). Intra-reader ICC was >0.7 for AVS, AVK, and inhomogeneity, and >0.9 for P10, P25, P50, P75, P90, mean, and SD (see Table 1).

3.2. Comparisons between soft tissue sarcomas and benign soft tissue tumors

There was no significant difference in age or sex ($P > .05$) between the soft tissue sarcoma (n=24, mean age=46.4 years, age range=28–64, male: female=11:13) and benign tumor groups (n=25, mean age=42.3 years, age range=25–60, male: female=12:13).

Benign soft tissue tumors and soft tissue sarcomas did not differ in P10, P25, P50, P75, P90, mean, or SD of density ($P > .05$, see Table 2). AVS, AVK, and inhomogeneity were significantly higher in soft tissue sarcomas versus benign soft tissue tumors ($P < .05$, see Table 2).

The area under the curve (AUC) was below 0.6 for P10, P25, P50, P75, P90, mean, and SD. AUC was 0.81, 0.83, and 0.84 for AVS, AVK, and inhomogeneity, respectively.

Figures 1 and 2 are examples of soft tissue sarcomas with relatively high AVK, AVS, and inhomogeneity. Figures 3–5 are

Table 1

Intra-reader and inter-reader reproducibility for histogram parameters were determined by calculating intra-class correlation coefficients.

ICC	P10	P25	P50	P75	P90	Mean	SD	AVS	AVK	Inhomogeneity
Intra	0.96	0.98	0.97	0.98	0.99	0.99	0.99	0.73	0.76	0.78
Inter	0.95	0.97	0.96	0.97	0.98	0.99	0.99	0.73	0.74	0.77

AVK = absolute value of kurtosis, AVS = absolute value of skewness, ICC = intra-class correlated coefficient, P10 = 10th percentile, P25 = 25th percentile, P50 = 50th percentile, P75 = 75th percentile, P90 = 90th percentile, SD = standard deviation.

Table 2

Histogram parameters were compared between soft tissue sarcomas and benign soft tissue tumors using a Mann–Whitney *U* test.

	P10	P25	P50	P75	P90	Mean	SD	AVS	AVK	Inhomogeneity
Soft tissue sarcoma	0.57	25.08	55.03	97.55	139.19	54.45	22.96	0.45	0.53	0.43
Benign soft tissue tumor	3.49	22.04	47.77	91.05	118.64	47.93	22.12	0.29	0.28	0.25
P	.69	.75	.46	.85	.68	.51	.98	.04	.02	.03

Median values were provided in the table for the histogram parameters.

AVK = absolute value of kurtosis, AVS = absolute value of skewness, P10 = 10th percentile, P25 = 25th percentile, P50 = 50th percentile, P75 = 75th percentile, P90 = 90th percentile, SD = standard deviation.

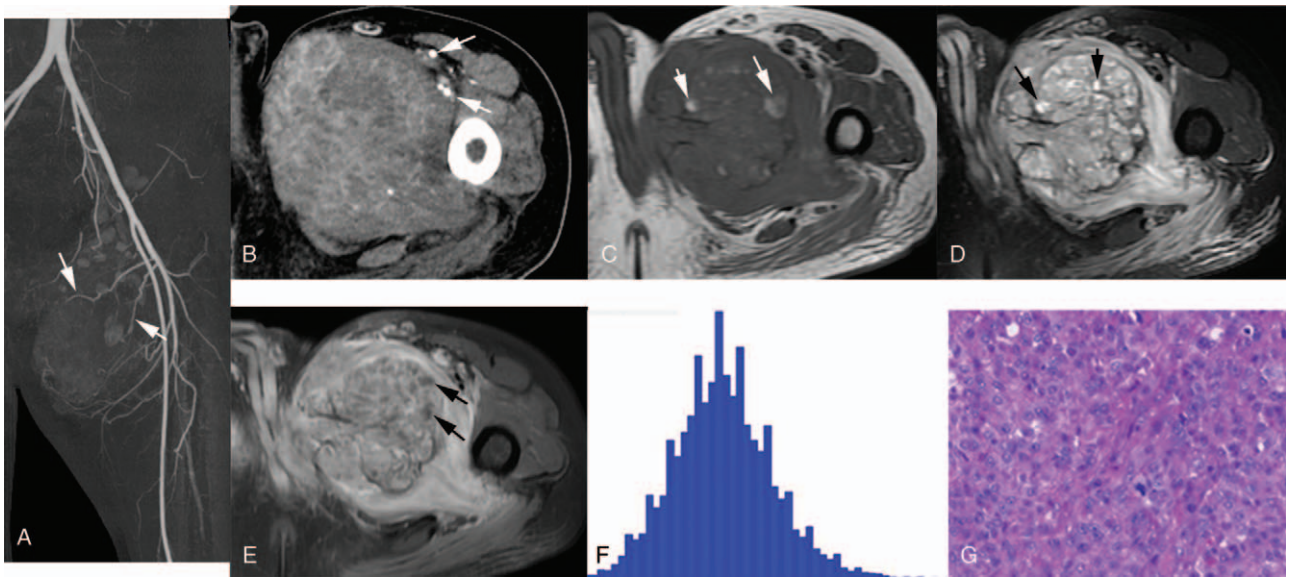

Figure 1. A 40-year-old man with a large soft tissue mass in the left thigh. Feeding arteries were well-depicted on maximum intensity projection CTA images (A, arrows). The tumor boundaries were not well-depicted on CTA source images (B), but the images clearly demonstrate tumor displacement of the regional arteries (B, arrows). Intra-tumor hemorrhage is seen on the T1-weighted MR images (C, arrows), while necrosis is better visualized on the T2-weighted images (D, arrows). Tumor enhancement was heterogeneous (E). Contrast-enhanced T1-weighted images also showed show multiple areas of necrosis (E, arrows). Kurtosis, skewness, and inhomogeneity derived from the histogram (F) were 0.94, 0.79, and 0.42, respectively. The pathology showed an epithelioid sarcoma (G).

examples of benign soft tissue tumor with relatively low AVK, AVS, and inhomogeneity.

4. Discussions

The current study investigated the feasibility of CTA-derived histogram analysis in distinguishing between soft tissue sarcomas from benign soft tissue tumors. The most important findings are as follows: the reproducibility of CTA histogram analyses is excellent; soft tissue sarcoma and benign soft tissue tumors differ in AVS, AVK, and inhomogeneity, but not in mean, SD, or percentile density measurements.

Histogram analysis of CT density is one of the most widely used CTTA methods.[23–25] Compared with basic ROI analysis, more parameters can be obtained with histogram analysis, such as percentiles, skewness, kurtosis, and inhomogeneity. Percentiles provide additional information regarding density distributions. Skewness and kurtosis reflect the extent of deviation from a normal distribution. Skewness, kurtosis, and inhomogeneity have been reported as additional valuable parameters reflecting tumor heterogeneity.[3,26,27]

Malignant tumors generally enhance more robustly than benign tumors due to greater neovascularity. CT density parameters derived from contrast-enhanced CT were expected to be higher in soft tissue sarcomas than in benign soft tissue tumors. However, no difference in histogram-derived CT density parameters was identified between the 2 groups. The most likely explanation is that the early tumor enhancement achieved with CTA only slightly elevated the overall tumor density. The standard deviation of CT density parameters also did not differ between the 2 groups, and the AUC for both mean and SD were poor (<0.6). Thus, basic analyses of mean/SD were not suitable for distinguishing between soft tissue sarcomas and benign soft tissue tumors.

The percentile values (P10–P90) also did not differ between soft tissue sarcomas and benign tumors. P10 likely represents voxels within areas of liquefied necrosis, as the absolute values were approximately the density of water. Both benign and malignant soft tissue tumors could have liquefied necrosis, reflecting similar P10 values. P90 most likely reflects intravascular enhancement as its absolute value was >100 HU for both groups. As enhanced vessels are present in both benign tumors and soft tissue sarcomas, P90 values also did not differ between the groups. Benign tumors and soft tissue sarcomas also did not differ in P50, which was close to the mean density of the tumor. AUC values were poor (<0.6) for P25 and P75. Thus, CT

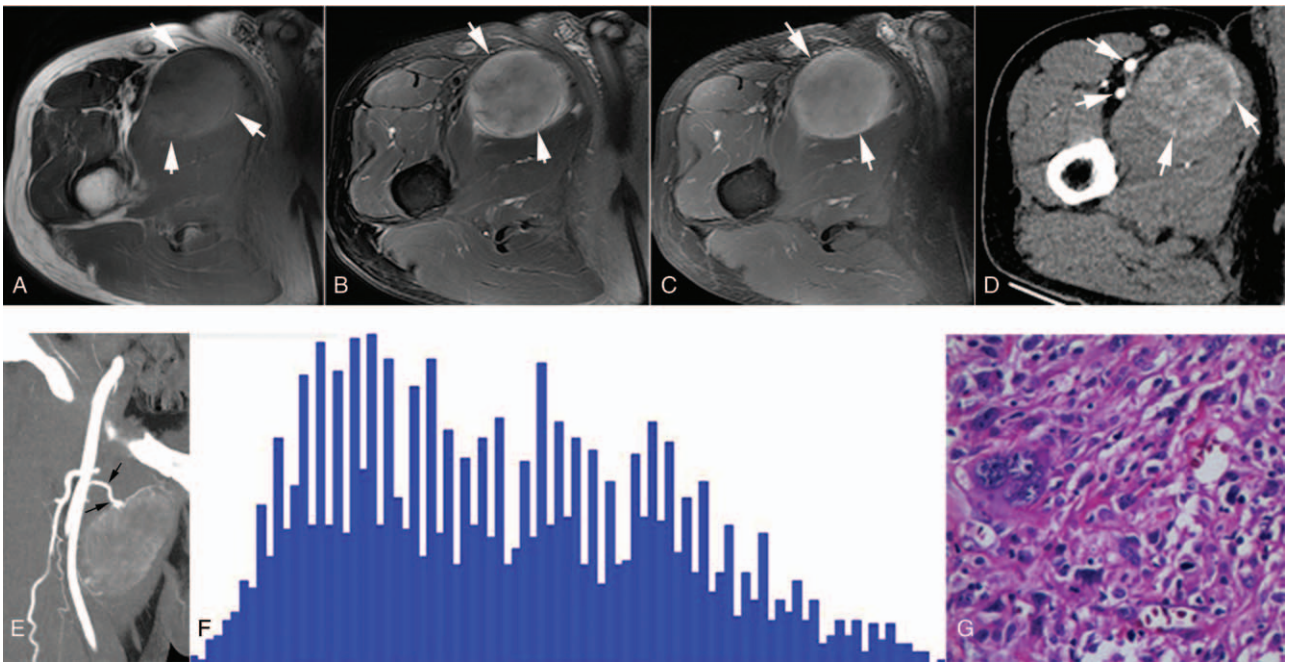

Figure 2. A 62-year-old man with a mass in the right thigh. The tumor was hyperintense on the T1-weighted MR image (A, arrows), and heterogeneously hyperintense on the T2-weighted image (B, arrows). The enhancement was heterogeneous on the contrast-enhanced T1-weighted image (C, arrows) and the CTA source image (D, arrows). The main arteries were free from tumor, and the feeding artery was well-depicted on reconstructed maximum intensity projection CTA images (E, arrows). Kurtosis, skewness, and inhomogeneity derived from the histogram (F) were –0.68, 0.48, and 0.54, respectively. The pathology showed a leiomyosarcoma (G). CTA = computed tomography angiography.

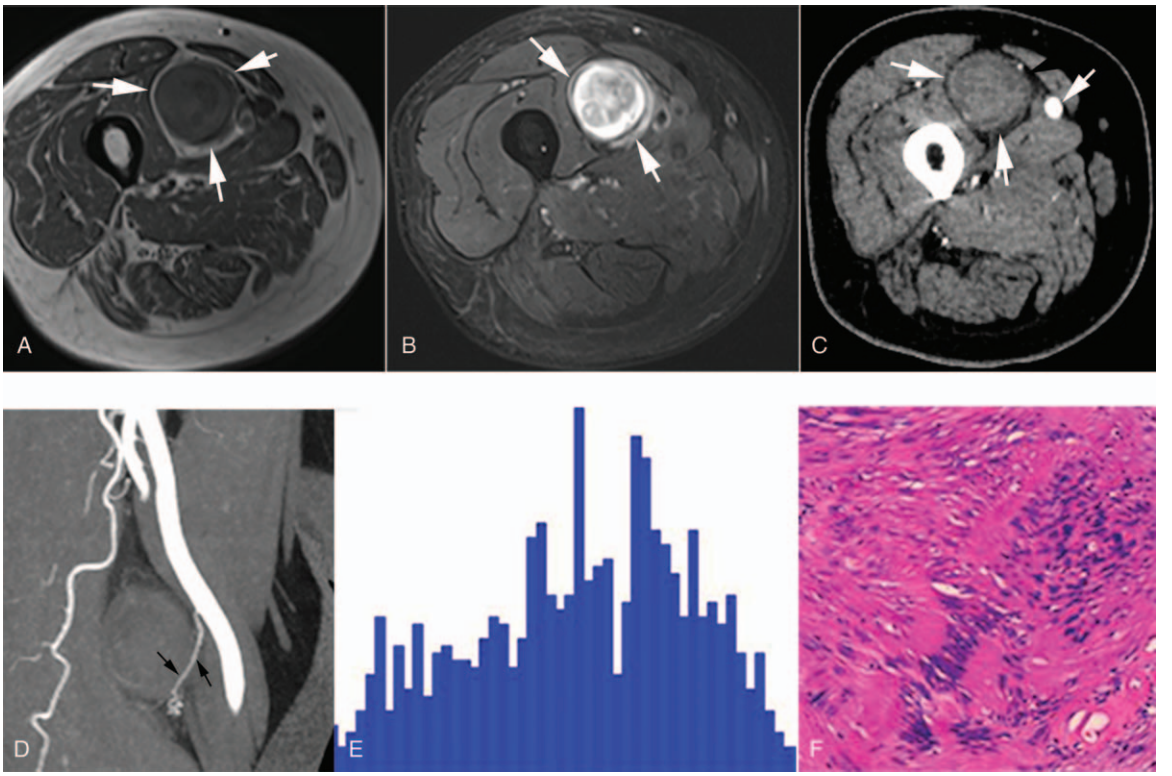

Figure 3. An 84-year-old man with a right thigh mass. T1 and T2-weighted MR images depicted the tumor (A, B, arrows). CTA was performed to better delineate tumor involvement of the adjacent femoral artery. The CTA image was superior to MR in confirming the lack of arterial invasion (C, arrows). The tumor feeding artery was also identified on a reconstructed maximum intensity projection CTA image (D, arrows). Kurtosis, skewness, and inhomogeneity derived from the histogram (E) were 0.15, 0.21, and 0.23, respectively. The pathology showed a schwannoma (F). CTA = computed tomography angiography.

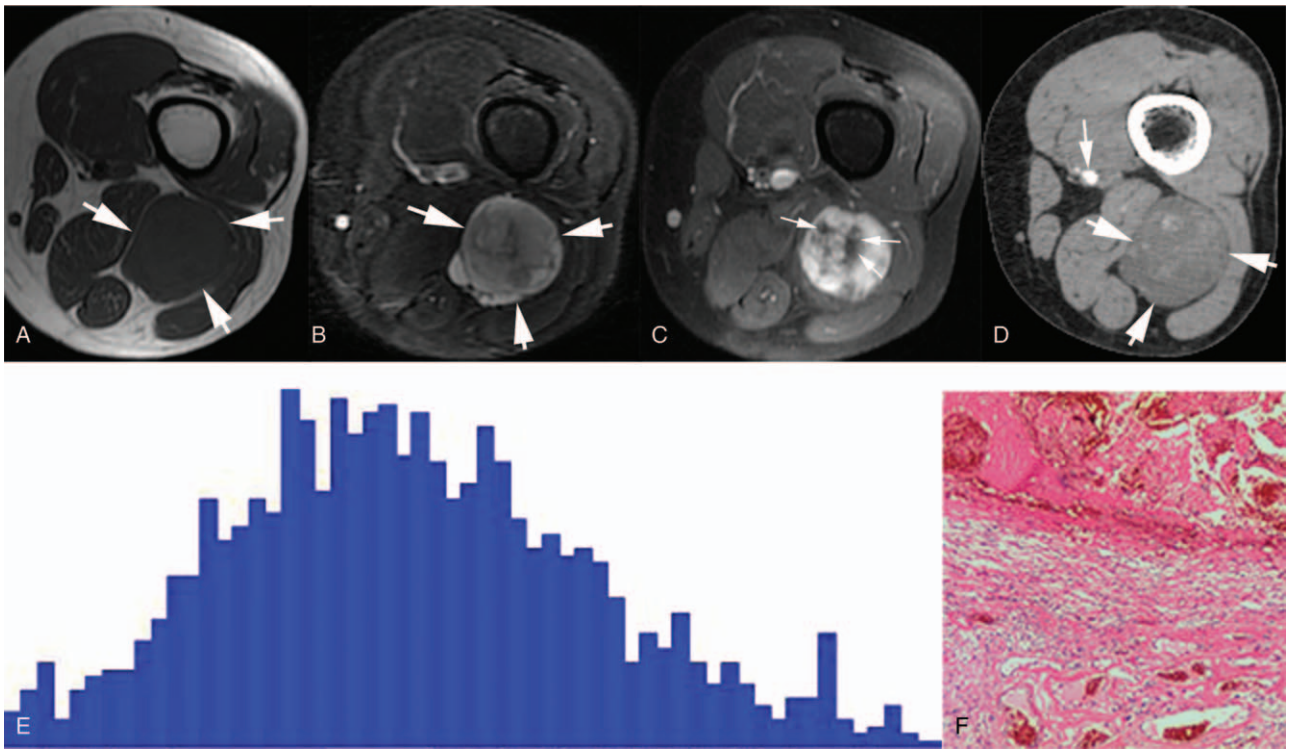

Figure 4. A 46-year-old woman with a left thigh mass. The tumor was isointense on T1-weighted MR (A, arrows) and hyperintense on T2-weighted MR (B, arrows). Contrast enhanced T1-weighted images depicted multiple mildly enhancing and non-enhancing lesions (C, arrows). The femoral artery was free from tumor (D, arrows). Kurtosis, skewness, and inhomogeneity derived from the histogram (E) were 0.31, 0.29, and 0.28, respectively. The pathology showed a hemangioma (F).

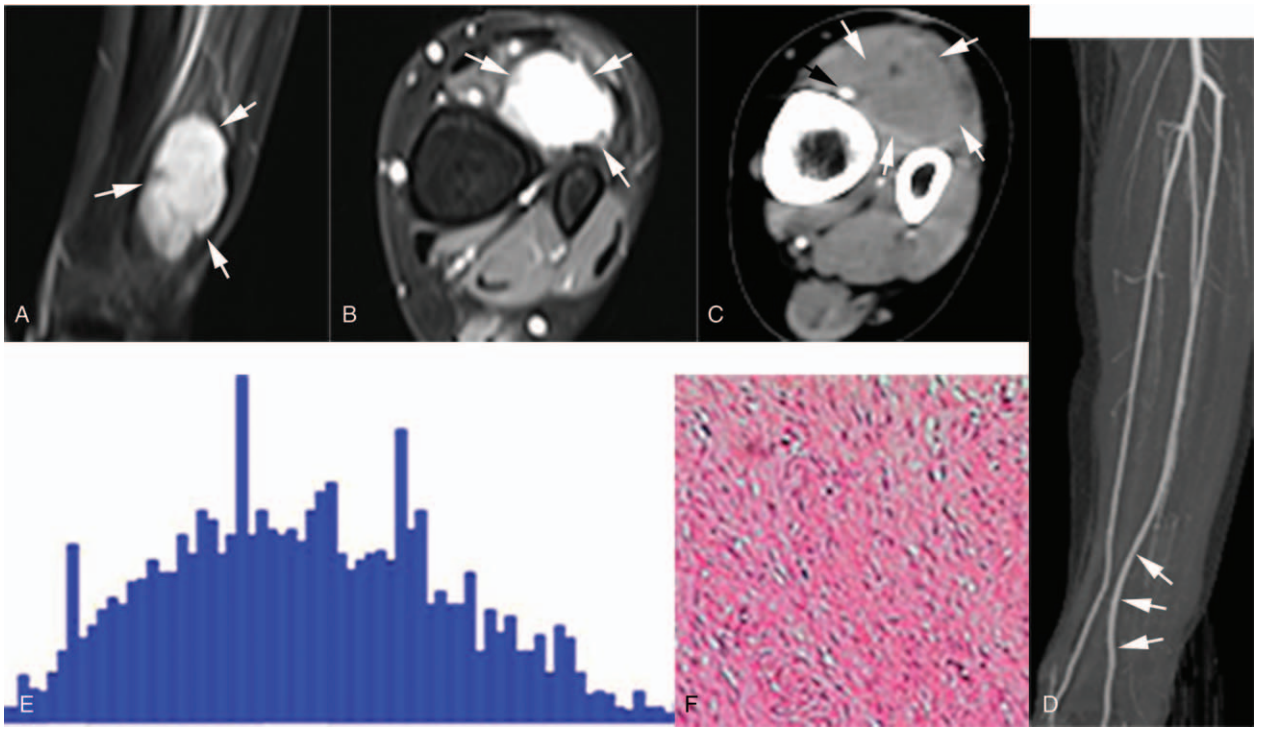

Figure 5. A 26-year-old woman with a mass in the left calf. The tumor boundary could be easily identified on both coronal (A, arrows) and axial (B, arrows) contrast-enhanced T1-weighted MR images, but was unclear on the CTA image (C, arrows). The medial displacement of the anterior tibial artery was better depicted on the reconstructed CTA image (D, arrows) compared with the CTA source image (C, black arrow). Kurtosis, skewness, and inhomogeneity derived from the histogram (E) were 0.17, 0.29, and 0.21, respectively. The pathology showed a fibroma (F). CTA = computed tomography angiography.

density percentiles (P10–P90) appear to not be suitable for discrimination of benign and malignant tumors.

Despite the inability of CTA-derived mean and percentile values to discriminate between benign and malignant tumors, histogram analysis of CTA data still proved valuable as the parameters of skewness, kurtosis, and inhomogeneity did allow for this differentiation. AUC for AVS, AVK, and inhomogeneity were all >0.8. The measurement reproducibility for these parameters was also excellent (ICC >0.7) for AVS, AVK, and inhomogeneity.

The distribution of CT densities may be normal or nearly normal in benign lesions, but as the current study supports, non-normal distributions are commonly found in malignant tumors.[28] Parameters that reflected the extent of deviation from a normal distribution (including AVK, AVS, and inhomogeneity) were significantly higher in soft tissue sarcomas compared with benign tumors. The most likely explanation for this is the complex structure and greater variety of pathological changes seen with sarcomas including areas of necrosis, hemorrhage, and calcification.

The current study has some limitations. First, the sample size was small, especially for the soft tissue sarcoma group. Soft tissue tumors in the lower extremity are uncommon, and CTA is not typically performed for small lower extremity tumors. Thus only 49 cases met the inclusion criteria over nearly 5 years. Larger multi-center studies are needed to validate the current results. Second, the histogram analyses were performed using CTA, not conventional contrast enhanced CT. Tumor enhancement extent may differ between the 2 tests. However, conventional contrast enhanced CT is seldom utilized for the assessment of soft tissue tumors in the lower extremity due to inadequate soft tissue resolution. Histogram analysis with MRI is an additional area of potential future research, but the current study was focused on CTTA. Third, the benign soft tissue tumor group consisted of several pathologically distinct entities. The sample size for each benign tumor group was too small to support separate statistical analysis, and thus all benign tumors were combined into one group. Optimally, a more direct comparison should be performed in future studies, such as fibrosarcoma versus fibroma.

In conclusion, skewness, kurtosis, and inhomogeneity derived from histogram analysis with CTA could be useful in distinguishing between soft tissue sarcomas and benign soft tissue tumors.

Author contributions

Conceptualization: Ruyi Xie, Gang Wu.
Data curation: Ruyi Xie, Gang Wu, Yitong Li, Bowen Hou, Xiaoming Li.
Formal analysis: Gang Wu, Yitong Li, Bowen Hou, Xiaoming Li.
Funding acquisition: Ruyi Xie, Gang Wu, Xiaoming Li.
Investigation: Gang Wu.
Methodology: Ruyi Xie, Gang Wu, Yitong Li, Bowen Hou, Xiaoming Li.
Project administration: Gang Wu, Bowen Hou, Xiaoming Li.
Resources: Gang Wu, Yitong Li, Xiaoming Li.
Software: Ruyi Xie, Gang Wu, Yitong Li, Xiaoming Li.
Supervision: Ruyi Xie, Gang Wu, Bowen Hou.
Validation: Gang Wu, Bowen Hou, Xiaoming Li.
Visualization: Ruyi Xie, Gang Wu, Xiaoming Li.
Writing – original draft: Ruyi Xie, Gang Wu, Xiaoming Li.
Writing – review & editing: Gang Wu, Xiaoming Li.

References

[1] Miller BJ. Use of imaging prior to referral to a musculoskeletal oncologist. J Am Acad Orthop Surg 2019;27:e1001–8.
[2] Hochman MG, Wu JS. MR imaging of common soft tissue masses in the foot and ankle. Magn Reson Imaging Clin N Am 2017;25:159–81.
[3] Choi IY, Yeom SK, Cha J, et al. Feasibility of using computed tomography texture analysis parameters as imaging biomarkers for predicting risk grade of gastrointestinal stromal tumors: comparison with visual inspection. Abdom Radiol 2019;44:2346–56.
[4] Cherezov D, Goldgof D, Hall L, et al. Revealing tumor habitats from texture heterogeneity analysis for classification of lung cancer malignancy and aggressiveness. Sci Rep 2019;9:4500.
[5] Feng Z, Shen Q, Li Y, et al. CT texture analysis: a potential tool for predicting the Fuhrman grade of clear-cell renal carcinoma. Cancer Imaging 2019;19:6.
[6] Feng C, Lu F, Shen Y, et al. Tumor heterogeneity in gastrointestinal stromal tumors of the small bowel: volumetric CT texture analysis as a potential biomarker for risk stratification. Cancer Imaging 2018; 18:46.
[7] Xu F, Ma X, Wang Y, et al. CT texture analysis can be a potential tool to differentiate gastrointestinal stromal tumors without, KIT, Exon 11 mutation. Eur J Radiol 2018;107:90–7.
[8] Nishio M, Nagashima C. Computer-aided diagnosis for lung cancer: usefulness of nodule heterogeneity. Acad Radiol 2017;24:328–36.
[9] Andersen MB, Harders SW, Ganeshan B, et al. CT texture analysis can help differentiate between malignant and benign lymph nodes in the mediastinum in patients suspected for lung cancer. Acta Radiol 2016;57:669–76.
[10] Zhang G, Yang Z, Gong L, et al. Classification of benign and malignant lung nodules from CT images based on hybrid features. Phys Med Biol 2019;64:125011.
[11] Deng Y, Soule E, Samuel A, et al. CT texture analysis in the differentiation of major renal cell carcinoma subtypes and correlation with Fuhrman grade. Eur Radiol 2019;29:6922–9.
[12] You MW, Kim N, Choi HJ. The value of quantitative CT texture analysis in differentiation of angiomyolipoma without visible fat from clear cell renal cell carcinoma on four-phase contrast-enhanced CT images. Clin Radiol 2019;74:547–54.
[13] Shi B, Zhang GM, Xu M, et al. Distinguishing metastases from benign adrenal masses: what can CT texture analysis do? Acta Radiol 2019;60:1553–61.
[14] Kuroda S, Itoh H, Yamagami T, et al. Angiomyolipoma arising in the thigh. Skeletal Radiol 2000;29:293–7.
[15] Pang LM, Roebuck DJ, Griffith JF, et al. Alveolar soft-part sarcoma: a rare soft-tissue malignancy with distinctive clinical and radiological features. Pediatr Radiol 2001;31:196–9.
[16] Cetinkaya OA, Celik SU, Kalem M, et al. Clinical characteristics and surgical outcomes of limb-sparing surgery with vascular reconstruction for soft tissue sarcomas. Ann Vasc Surg 2019;56:73–80.
[17] Nishinari K, Krutman M, Aguiar Junior S, et al. Surgical outcomes of vascular reconstruction in soft tissue sarcomas of the lower extremities. J Vasc Surg 2015;62:143–9.
[18] Wu G, Yang H, Li X. Feeding arteries and arteriovenous shunt for discrimination of soft tissue tumors. Medicine (Baltimore) 2019;98: e16346.
[19] Schlett CL, Maurovich-Horvat P, Ferencik M, et al. Histogram analysis of lipid-core plaques in coronary computed tomographic angiography: ex vivo validation against histology. Invest Radiol 2013;48:646–53.
[20] Kim SK, Jee WH, Lee AW, et al. Haemorrhagic low-grade fibromyxoid sarcoma: MR findings in two young women. Br J Radiol 2011;84: e146–50.
[21] Koh SH, Choe HS, Lee IJ, et al. Low-grade fibromyxoid sarcoma: ultrasound and magnetic resonance findings in two cases. Skeletal Radiol 2005;34:550–4.
[22] Wang CS, Duan Q, Xue YJ, et al. Giant cell tumour of tendon sheath with bone invasion in extremities: analysis of clinical and imaging findings. Radiol Med 2015;120:745–52.
[23] Kawashima Y, Fujita A, Buch K, et al. Using texture analysis of head CT images to differentiate osteoporosis from normal bone density. Eur J Radiol 2019;116:212–8.
[24] Lim HK, Ha HI, Park SY, et al. Comparison of the diagnostic performance of CT Hounsfield unit histogram analysis and dual-energy X-ray absorptiometry in predicting osteoporosis of the femur. Eur Radiol 2019;29:1831–40.

[25] Tsubakimoto M, Yamashiro T, Tamashiro Y, et al. Quantitative CT density histogram values and standardized uptake values of FDG-PET/CT with respiratory gating can distinguish solid adenocarcinomas from squamous cell carcinomas of the lung. Eur J Radiol 2018;100:108–15.
[26] Lu J, Hu D, Tang H, et al. Assessment of tumor heterogeneity: differentiation of periampullary neoplasms based on CT whole-lesion histogram analysis. Eur J Radiol 2019;115:1–9.
[27] Digumarthy SR, Padole AM, Lo Gullo R, et al. CT texture analysis of histologically proven benign and malignant lung lesions. Medicine (Baltimore) 2018;97:e11172.
[28] Choi EK, Im JJ, Park CS, et al. Usefulness of feature analysis of breast-specific gamma imaging for predicting malignancy. Eur Radiol 2018; 28:5195–202.